Stopped-flow spectrophotometric analysis of intermediates in the peroxo-dependent inactivation of cytochrome P450 by aldehydes

By: Gregory M. Raner, Andrew J. Hatchell, Patrick E. Morton, David P. Ballou, Minor J. Coon

Raner, G.M. A.J. Hatchell, P.E. Morton, D.P. Ballou, and M.J. Coon. Stopped-Flow Spectrophotometric Analysis of Intermediates in the Peroxo-Dependent Inactivation of Cytochrome P450 by Aldehydes. J. Inorg. Biochem. 81: 153-160 (2000). DOI: 10.1016/S0162-0134(00)00098-2

Abstract:

The reaction of hydrogen peroxide and certain aromatic aldehydes with cytochrome $P450_{BM3}$-F87G results in the covalent modification of the heme cofactor of this monooxygenase. Analysis of the resulting heme by electronic absorption spectrophotometry indicates that the reaction in the BM3 isoform is analogous to that in $P450_{2B4}$, which apparently occurs via a peroxyhemiacetal intermediate [Kuo et al., Biochemistry, 38 (1999) 10511]. It was observed that replacement of the Phe-87 in the $P450_{BM3}$ by the smaller glycyl residue was essential for the modification to proceed, as the wild-type enzyme showed no spectral changes under identical conditions. The kinetics of this reaction were examined by stopped-flow spectrophotometry with 3-phenylpropionaldehyde and 3-phenylbutyraldehyde as reactants. In each case, the process of heme modification was biphasic, with initial bleaching of the Soret absorbance, followed by an increase in absorbance centered at 430 nm, consistent with meso-heme adduct formation. The intermediate formed during phase I also showed an increased absorbance between 700 and 900 nm, relative to the native heme and the final product. Phase I showed a linear dependence on peroxide concentration, whereas saturation kinetics were observed for phase II. All of these observations are consistent with a mechanism involving radical attack at the γ-meso position of the heme cofactor, resulting in the intermediate formation of an isoporphyrin, the deprotonation of which produces the γ-meso-alkyl heme derivative.

Keywords:

Cytochrome P450; Aldehydes; Heme; Isoporphyrin; Kinetics

Article:

1. INTRODUCTION

The proposed catalytic cycle of cytochrome P450 consists of multiple reactive oxygen species, each capable, in theory, of initiating substrate oxidation. The oxenoid iron (Fe^{V}=O) intermediate has gained widespread acceptance as an oxygenating agent. This intermediate, proposed over 25 years ago, is central to the oxygen-rebound mechanism, which accounts for the many stereochemical and regiochemical results observed in cytochrome P450-catalyzed hydroxylation reactions [1–3]. Further studies of alcohol [4] and aldehyde [5] oxidation and N-oxygenation [6] reactions also point to an analogous cytochrome P450 intermediate during catalysis. In fact, it is widely assumed that the majority of oxidative chemical transformations effected by cytochrome P450 enzymes occur via the obligatory formation of the oxenoid iron intermediate. This intermediate, referred to as compound I, has been well characterized in the peroxidases [7], a related class of enzymes that, like P450, contain a heme prosthetic group. Direct observation of the ‘compound I-like’ intermediate in the $P450_{CAM}$ reaction cycle was first accomplished through the use of stopped-flow experiments in which m-chloroperoxybenzoic acid was used as an oxygen surrogate, by-passing the electron transfer and oxygen binding steps in the cycle [8]. More recently, an X-ray crystal structure of an apparent oxo-ferryl

intermediate of $P450_{CAM}$, the decomposition of which results in hydroxylated camphor, has appeared in the literature [9], leaving little doubt that oxenoid iron plays a critical role in catalysis.

In 1982, Akhtar et al. [10] proposed that a ferric-peroxo intermediate formed prior to the oxenoid iron was directly responsible for the terminal step in the demethylation of androgens to estrogens by the enzyme P450-aromatase. Using model substrates intended to mimic the structure of the physiological androgens, Roberts et al. [11] and Vaz et al. [12] showed that purified liver microsomal enzymes were able to catalyze the analogous deformylation of xenobiotic aldehydes. Subsequent studies involving the use of site-directed mutagenesis showed that aldehyde deformylation and substrate hydroxylations by $P450_{2B4}$ utilize different activated oxygen intermediates in catalysis, with deformylation occurring, most likely, via a nucleophilic attack of a ferric peroxo species at the electropositive carbonyl carbon to form a transient peroxohemiacetal [13] (Scheme I).

Studies by Raner et al. [5] involving aromatic aldehydes showed that for a single substrate, both oxenoid-iron and peroxo-iron metabolic routes are available. With certain aldehydes, heme modification was observed, and subsequent studies by Kuo et al. [14] indicated that the modification results from addition of a deformylated reaction product to the γ-meso position of the heme cofactor in $P450_{2B4}$.

Although indirect chemical evidence for the occurrence of the peroxy-hemiacetal intermediate in aldehyde deformylation is compelling, no direct evidence for its existence has been offered. In this study we have used stopped-flow spectrophotometry in an attempt to directly observe intermediates in the peroxide-dependent alkylation of the heme cofactor in cytochrome P450 by the aromatic aldehydes 3-phenylpropionaldehyde (3-PP) and 3- phenylbutyraldehyde (3-PB). We have chosen to work with the bacterial enzyme $P450_{BM3}$ because it offers several advantages over the liver microsomal counterparts; in particular, the enzyme is cytosolic and can be easily purified from the recombinant strain of E. coli in which it is produced. The X-ray crystal structure of $P450_{BM3}$ has been solved, providing detailed structural information regarding substrate access and potential steric interactions within the active site [15]. Of the five bacterial P450s for which X-ray structural data are available, the BM3 isoform is the best model for the microsomal enzymes on the basis of its utilization of an analogous cytochrome P450 reductase redox partner. None of the other bacterial enzymes accept electrons from this type of flavoprotein. Finally, the BM3 enzyme is a functional fusion protein combining the P450 oxygenase enzyme and reductase in a single poly- peptide, which eliminates the necessity for dual purification procedures and subsequent reconstitution.

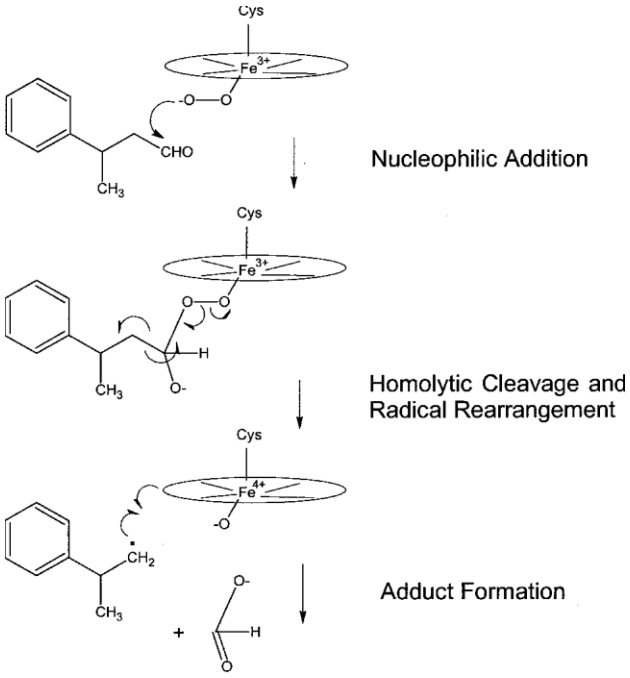

Scheme I.

Although advantageous in many ways, the use of BM3 in this study presented several obstacles. The native BM3 is a fatty acid hydroxylase with a correspondingly selective active site structure. The crystallographic data indicate that a phenylalanine residue at position 87 controls substrate entry into the active site cavity, which could preclude the use of the bulky aromatic aldehydes chosen for this study. Graham-Lorence et al. [16] first reported on a mutant form of BM3 in which the Phe87 residue was replaced by site-directed mutagenesis with a Val. This mutation altered the regiospecificity of the enzyme, presumably by allowing deeper penetration of the fatty acid substrate into the heme pocket. In addition, Schwaneberg et al. [17] reported higher rates of hydroxylation of p-nitrophenoxydodecanoic acid using the F87A mutant of BM3 relative to the wild- type form. We have therefore chosen to work with an analogous mutant form, F87G, in which Gly was the replacement for Phe. The complete removal of the aromatic side chain was expected to facilitate binding of bulkier substrates. An additional concern was the finding of Davis et al. [18] that fatty aldehyde substrates were oxidized to the corresponding diacids by P450BM3 with no observed deformylation products in reactions that utilized NADPH and molecular oxygen in catalysis. The study did not, however, examine the use of hydrogen peroxide as an oxygen donor. Previous studies using the liver enzymes suggest that the use of peroxide can enhance the rate of deformylation relative to other oxidative pathways [5]. To test whether $P450_{BM3}$ can catalyze deformylation reactions using hydrogen peroxide as an oxygen source was one of the objectives of the current study.

2. EXPERIMENTAL SECTION

2.1. Chemicals

The compounds 3-phenylpropionaldehyde and 3- phenylbutyraldehyde were purchased from Sigma (St. Louis, MO). All reagents used in the growth and induction of E. coli were from Fisher. Q-Sepharose and 2',5'-ADP agarose used for enzyme purification were from Pharmacia (Piscataway, NJ).

2.2. Enzyme preparations

Cytochrome $P450_{BM3}$-F87G was expressed in E. coli using a clone generously provided by Dr. David Mullin, Tulane University. Cells were grown in TB media at room temperature to an optical density of nearly 3.0, with shaking at 120 rev./min. Induction was accomplished by addition of 0.15 g/l IPTG, and the cells were incubated an additional 6–24 h at room temperature with reduced shaking (70 rev./min). Following enzymatic lysis, and sonication in 50 mM phosphate buffer (pH 7.4), 0.1 mM EDTA, containing 20% glycerol, the cytosolic material was separated from the cell debris by centrifugation (2.5 h at 54,000Xg). Purification of the wild-type and F87G mutant were carried out as described previously [19]. Approximately 50 to 100 mg of highly purified enzyme were produced per l bacterial culture. Enzyme concentrations were determined as described by Omura and Sato [20] using e_{450}=96 mM^{-1}.

2.3. Stopped-flow experiments

Experiments were carried out at 22°C using a Hi-Tech Model SF-61 stopped-flow spectrophotometer equipped with an MG6000 diode array. The integration time for each spectrum was 10 ms, with the time interval between scans determined by the duration of the individual experiment. Data were collected using Hi-Tech software and hardware installed on a DX2 Gateway 2000 66 MHz computer. From the diode array data, single wavelength traces at 418, 427, and 434 nm were extracted and analyzed by a two- sequential exponential fitting routine contained in the Hi-Tech software.

Reactions were initiated by the rapid mixing of a solution containing 6.0 µM cytochrome $P450_{BM3}$-F87G, 2.5 mM aldehyde, and 100 mM phosphate buffer (pH 7.4) with an equal volume of a solution containing 100 mM phosphate buffer (pH 7.4) and various concentrations of hydrogen peroxide. Two different aldehydes were examined in this study, 3-PP and 3-PB, with a range of hydrogen peroxide concentrations from 100 µM to 600 µM.

2.4. Purification and analysis of the modified hemes

$P450_{BM3}$-F87G (20 µM) was incubated with 100 µM H_2O_2 in the presence of 2.5 mM 3PB at 12°C for 15 min in 25 ml of 100 mM phosphate buffer (pH 7.4). Reactions were monitored spectrally at 434 nm to ensure complete conversion of wild-type heme to the corresponding modified derivative. The sample was bound to a Q-Sepharose (Pharmacia) anion exchange column equilibrated in 100 mM phosphate (pH 7.4) to remove excess aldehyde and unreacted H_2O_2. After the column had been washed with five volumes of 50 mM phosphate buffer, pH 7.4, the modified enzyme was eluted using 400 mM phosphate buffer, pH 7.4. The enzyme was precipitated by acidification to pH 3.0 using TFA, and the solid was collected by centrifugation. Under these conditions, the heme remained attached to the protein, while the flavins were released into the supernatant solution. Treatment of the pellets with 100% acetonitrile, containing 0.1% TFA, resulted in nearly complete extraction of the heme. Acetonitrile was evaporated and the resulting pellet was dissolved in 5.0 ml 50:50 acetonitrile:H_2O containing 0.1% TFA. The sample was injected onto a Higgins HAIsil C_{18} HPLC column (250X 4.6 mm), using a Rheodyne 7012 injector valve with 5.0 ml injection loop, at a flow rate of 1.0 ml/min. The HPLC system consisted of an LC-10AT dual pumping unit, an SCL-10A controlling unit, an FCV-10AL quaternary mixing chamber, a DGU-14A in-line degassing unit, an SPD-M10A diode array detector, and an SIL-10A autosampler, all interfaced to an Ast Bravo LC 5166M computer operating with a CLASS -VP automated software system. The mobile phase for this sample was 50:50 acetonitrile:H_2O, containing 0.1% TFA. Under these conditions, the retention time of the modified heme was 18.6 min, whereas that of the native cofactor was 10.1 min. The sample was recovered and the 50% acetonitrile solution was diluted 1:3 with H_2O and passed through a C_{18} reversed phase solid phase extraction device. The heme was bound tightly to this column under these conditions. The column was washed with 50 volumes of 40:60 and 50:50 acetonitrile:H_2O mixtures (both containing 0.1% TFA), the heme was eluted in 100% methanol with 0.1% TFA. Heme purified by this procedure did not appear to be altered during the extraction procedure. To confirm this, we injected a 50-µl sample of the enzyme, modified by H_2O_2 and 3PB treatment, directly onto the HPLC column under the conditions described above. We then injected a 50-µl sample of the modified heme we obtained by the purification method described. The HPLC retention times and absorption spectra of the alkylated hemes were the same.

The effect of aldehyde structure on retention time was examined using the aldehydes phenylacetaldehyde (PA), 3PP, and 4-phenylbutyraldehyde (4PB). The reaction of BM3-F87G with each aldehyde was carried out as described for 3PB above, and the resulting modified enzymes were injected directly onto a C_{18} HPLC column with a mobile phase of 60:40 acetonitrile:H_2O containing 0.1% TFA at a flow rate of 1.0 ml/min.

For the determination of the extinction coefficient of the modified heme, samples were taken directly from an analytical HPLC preparation in the mobile phase described previously, and examined by atomic absorption spectroscopy (Perkin Elmer 272 Atomic Absorption Spectrometer). The ε_{408} was determined using the combined atomic and electronic absorption data.

Electronic absorption spectra for the wild-type, and modified hemes, along with their respective holo-enzymes were recorded on a HP8453 diode array spectrophotometer. All spectrophotometric, kinetic, and chromatographic data were then imported into Slidewrite (Advanced Graphics Software Inc.).

3. RESULTS

3.1. Characterization of the modified hemes

Addition of 100 µM hydrogen peroxide to cytochrome $P450_{BM3}$-F87G in the presence of saturating levels of the aromatic aldehydes 3-PP and 3-PB resulted in the formation of an enzyme species with its Soret peak shifted from 418 nm to 430 nm (Fig. 1). Wild-type $P450_{BM3}$ did not undergo the same spectral changes under these conditions, but exhibited only a rather slow loss of heme absorbance (data not shown). The shift in the Soret peak of the F87G mutant enzyme results from the chemical modification of the heme group and corresponding spectral changes for the free heme (Fig. 2). The λ_{max} for wild-type heme is 398 nm, whereas the heme derivatives generated in this study show λ_{max} values of 408 nm. HPLC analysis of the free modified and native hemes indicated a relationship between the size of the aldehyde used in the experiment and the retention time of

the product heme. For example, we chose a series of unbranched aromatic aldehydes that differed only in the number of methylene carbons in the chain. Retention times of 6.4, 8.0, 10.9, and 12.3 min were observed for the native, PA, 3PP, and 4PB modified hemes, respectively. This is consistent with previous studies involving the rabbit liver microsomal enzyme $P450_{2B4}$, in which a series of aldehydes with different molecular weights were examined [5]. The heme produced in the reaction with 3-PB was analyzed by atomic absorption spectroscopy to determine the molar extinction coefficient. A sample with an A_{408}=0.805 was shown to have an iron content of 7.7 µM, giving an ε_{408} of 104,000 M^{-1} cm^{-1}.

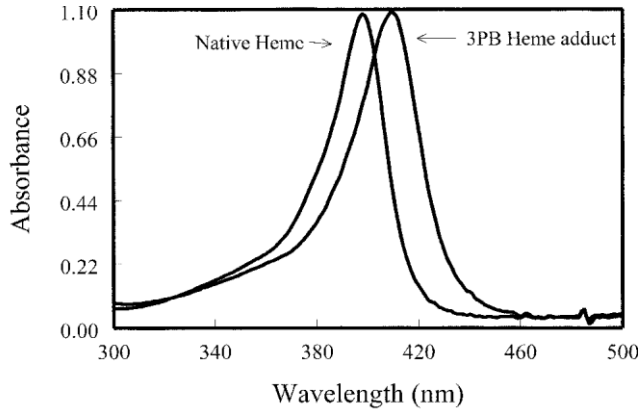

Fig. 2. Electronic absorption spectrum for the purified native heme and the heme derivative generated in the reaction of $P450_{BM3}$-F87G with 3-PB and 300 µM H_2O_2. Absorption maxima for the native and modified hemes are 398 nm and 408 nm, respectively. Spectra were recorded using the HPLC diode array detector, thus the solvent in each case was the mobile phase for chromatography (50:50 acetonitrile:H_2O, with 0.1% TFA).

3.2. Stopped-flow experiments

The reaction of $P450_{BM3}$-F87G with 3-PB proceeded in at least two phases as indicated by the kinetic trace shown in Fig. 3, illustrating the change in absorbance at 426 nm within the first 90 s after mixing (426 nm was chosen because it best illustrated the biphasic nature of the reaction). Phase I was characterized by a decrease in absorbance over nearly the entire wavelength range. An increase in absorbance was observed in the 700–900 nm range during this first phase of the reaction (Fig. 4). Phase II consisted of an increase in absorbance centered at 430 nm, with a loss of the absorbance near 850 nm that originated in phase I. The spectral changes between 320 and 700 nm for each phase, as a function of time, are shown in Fig. 5. The temperature at which the experiments were carried out significantly effected the rates of both

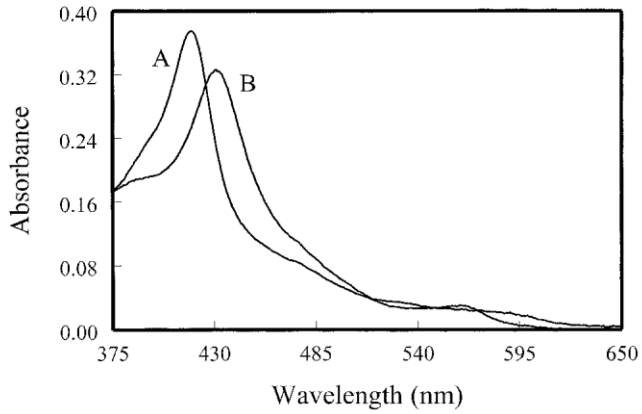

Fig. 1. Electronic absorption spectra of (A) $P450_{BM3}$-F87G in 100 mM phosphate buffer, pH 7.4, containing 1.25 mM 3-PB and (B) same sample 20 min after addition of 300 µM H_2O_2 at 22°C. The λ_{max} for the enzyme in A is 418 nm and that for B is 432 nm.

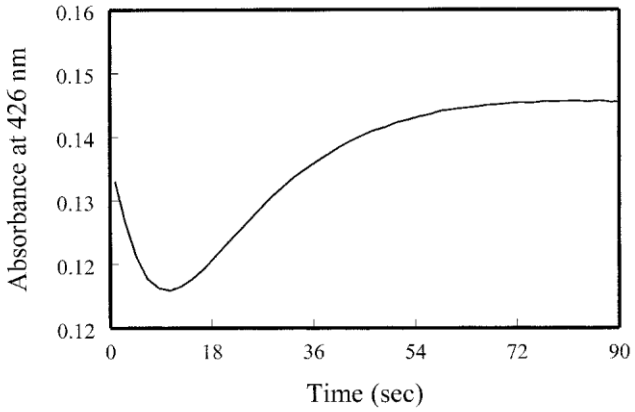

Fig. 3. Kinetic trace of the reaction of $P450_{BM3}$-F87G with 1.25 mM 3-phenylbutyraldehyde and 600 μM H_2O_2 monitored at 426 nm. The reaction was carried out at 22°C. Phase I occurred between 0 and 12 s, and phase II was complete within 1.0 min.

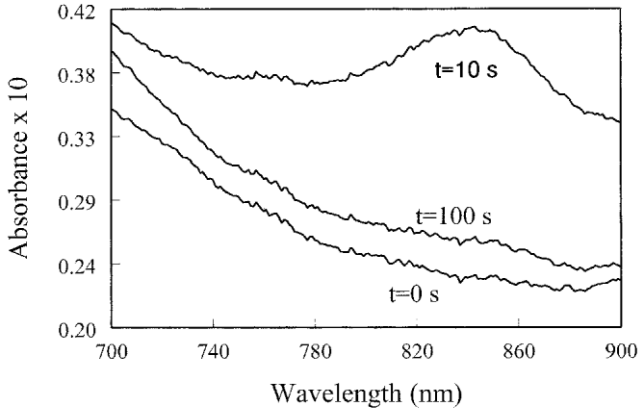

Fig. 4. Absorbance change in the 700–900 nm range during the reaction of $P450_{BM3}$-F87G with 3-phenylbutyraldehyde and 600 μM H_2O_2 at 22°C. Spectra were recorded at 0, 10, and 100 s after addition of H_2O_2.

phases, as well as the amount of heme adducts formed. For example, higher reaction temperatures appeared to result in greater amounts of heme degradation (not shown). Experi-

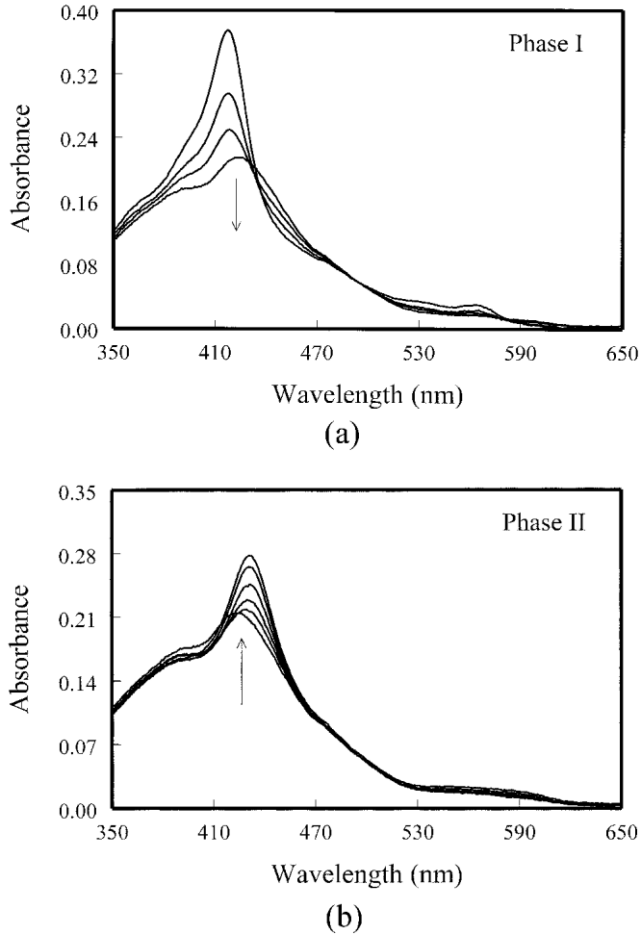

Fig. 5. Spectral changes in the Soret peak during the two phases associated with heme adduct formation with 1.25 mM 3-PB and 300 μM H_2O_2 in 100 mM phosphate buffer, pH 7.4, at 22°C. (a) Phase I corresponds to 0–20 s. (b) Phase II corresponds to 20–100 s. Arrows indicate changes with increasing time.

ments were therefore carried out at 22°C. The effects of light on the reaction were also examined; by reducing the light intensity using a stainless wire mesh as a filter, and increasing the integration time from 1.25 to 10 ms, we were able to reduce the amount of spectral bleaching without loss of sensitivity. With 3PP, the observed rate constants, k_1 and k_2, associated with phases I and II, respectively, were sensitive to hydrogen peroxide concentration. As the concentration of 3PP was varied from 100 to 600 μM, k_1 increased from 0.037 to 0.124s^{-1}, and k_2 increased from 0.012 to 0.044 s^{-1} as determined at 427, 418 and 434 nm. Although k_1 displayed a linear dependence on H_2O_2 concentration, k_2 showed saturation behavior. Qualitatively, our results with 3-PP were identical to those obtained with the branched aldehyde; however, with 3PB, the k_2 values were somewhat smaller (0.017 s^{-1} at 600 μM H_2O_2), which had the effect of increasing the half-life of the spectral intermediate. Plots of observed k_1 values vs. H_2O_2 concentration for 3PP and 3PB are shown in Fig. 6a. Fig. 6b shows double reciprocal plots of the data for k_2, from which we can extrapolate values for k_2 at infinite H_2O_2 concentration, or theoretical maximum values for k_2. For 3PP, this value was approximately sixfold higher than for 3PB.

4. DISCUSSION

Heme adduct formation in cytochrome P450, as a consequence of exposure to aldehydes and hydrogen peroxide, has been examined previously with the microsomal isoform 2B4 [5,14]. In these studies it was shown that the aldehyde undergoes loss of the carbonyl carbon and the resulting radical species attacks the heme prosthetic group at the γ-meso position. In the current study, we have examined the analogous heme modification process in the bacterial isoform $P450_{BM3}$ (F87G mutant) using stopped-flow spectrophotometry in an attempt to characterize reaction intermediates. That $P450_{BM3}$-F87G is capable of this type of transformation

was evident from the spectral changes accompanying treatment with H_2O_2 and 3PP. We have confirmed that Phe-87 prevents binding of aromatic substrates by our observation that analogous spectral changes do not occur in the wild-type enzyme under identical reaction conditions.

Modification of the heme by an aldehyde-derived species was verified using several different structurally related aldehydes including PA, 3PP, and 4PB. Although each of the aldehydes produced a heme adduct in the presence of H_2O_2 and $P450_{BM3}$-F87G, and each heme adduct had a λ_{max} of 408 nm, the retention times of the adducts by HPLC correlated strongly with the size of the parent aldehyde, with larger more hydrophobic compounds producing heme adducts with longer retention times.

Spectral analysis of the modified heme cofactor generated in $P450_{BM3}$-F87G strongly suggests a mechanism

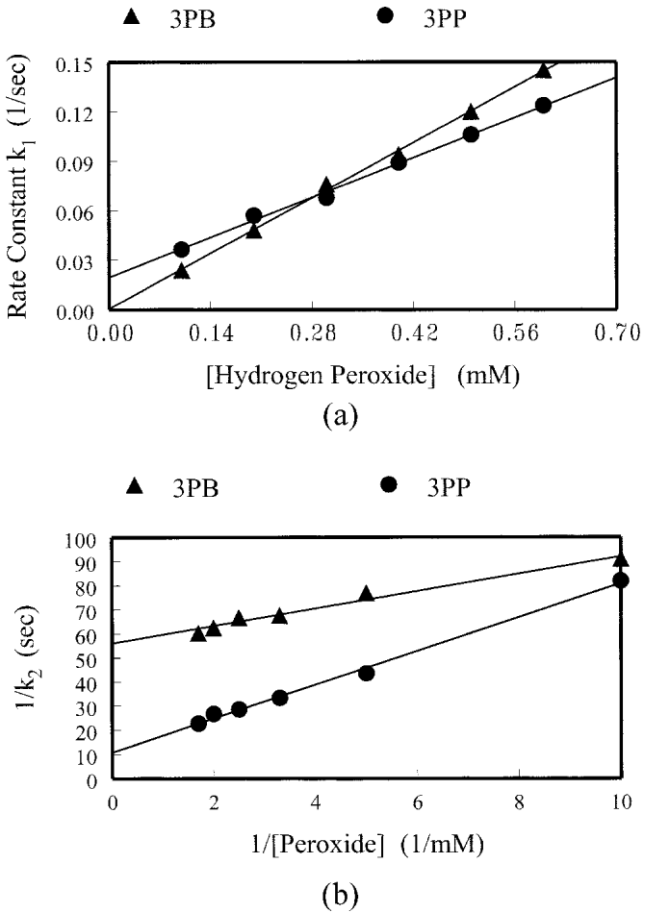

Fig. 6. Dependence of the observed rate constants for the reaction of $P450_{BM3}$-F87G with 3PB or 3PP on hydrogen peroxide concentration. (a) Effects of increasing H_2O_2 concentration on k_1. Calculated rate constants were 1.4×10^{-2} min^{-1} μM^{-1} and 1.0×10^{-2} min^{-1} μM^{-1} for 3PB and 3PP, respectively. (b) Due to saturation behavior, k_2 vs. H_2O_2 was plotted in double reciprocal format giving theoretical first-order k_2 values of 1.1 and 6.0 min^{-1} for 3PB and 3PP, respectively. Experiments were carried out as described in Section 2.

involving peroxo-iron. For example, Kuo et al. [14] showed that with $P450_{2B4}$, aldehydes can be activated by either the peroxo-pathway or the oxenoid iron pathway to form heme adducts. The two products are distinct, however, in their electronic absorption properties, with the peroxo-derived adduct possessing a maximum absorbance at 408 nm, vs. 402 nm for the oxenoid-iron-derived species. The adducts described in the current paper all have a λ_{max} of 408 nm. The most likely position of attack, on the basis of the known crystal structure of the BM3 enzyme, is the γ-meso carbon, just as in $P450_{2B4}$. For example, Fig. 7 shows the active site structure of $P450_{BM3}$ based on the crystal studies of Li and Poulos [15] (PDB file 2BMH). In the F87G mutant, removal of the bulky aromatic ring of Phe leaves a void in the active site. Aromatic substrates such as 3PP or 3PB might

be expected to effectively fill this void in the enzyme. Distances between the phenyl ring carbons on Phe 87 in the wild-type enzyme and the heme γ-meso position range from

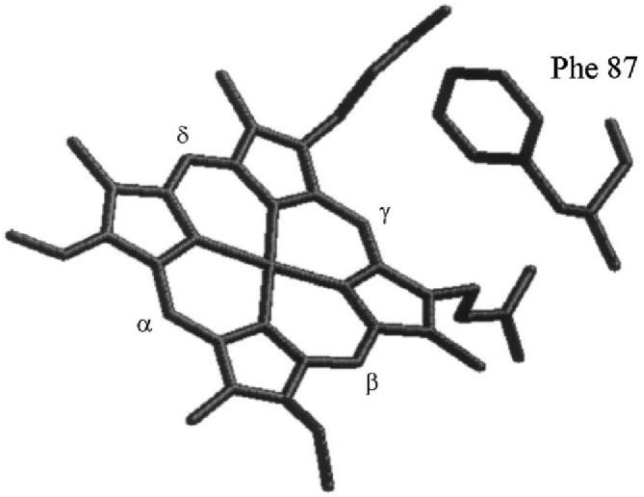

Fig. 7. X-ray crystal structure showing the relationship of Phe-87 to the heme group in wild-type $P450_{BM3}$. Structural coordinates were obtained from Brookhaven Protein Data Bank, file BMH2.PDB, and are based on the crystal structure of Li and Poulos [15].

3.86 A, for the Phe-ε-carbon facing the heme, to 6.28 Å, for the Phe-δ-carbon facing away from the heme. None of the other heme meso carbon atoms lie within 5.9 Å of any of the phenyl ring positions, and most are more than 7 Å away. Therefore, based on proximity, the most likely site for attachment of the phenylethyl radical, generated in the deformylation of 3PP, would be the γ-meso position of the heme.

We used stopped-flow spectrophotometry to examine the physical properties of intermediates in the reaction of aldehydes and H_2O_2 with $P450_{BM3}$-F87G. Two aldehydes were chosen for the study, as each could be used to generate a heme adduct in high yield (>80%), and heme degradation in these samples was minimal. The reaction with both aldehydes was biphasic, with the first phase consisting of a general bleaching of the spectrum in the visible region. The bleached spectrum is consistent with a heme that has lost some of its aromaticity, similar to compound I, in which a π-electron has been removed from the porphyrin macrocycle. Unlike compound I, however, this intermediate displays a maximum absorbance at 426 nm rather than 367, as reported by Egawa et al. [11]. Furthermore, absorbance increases in the 700–900 nm region, as observed in this experiment, have been associated with isoporphyrin spectra [21], but not P450 compound I, which has an absorption band centered at 694 nm. An isoporphyrin intermediate (Fig. 8) has been proposed in the reaction of HRP with cyclopropanone hydrate and with alkyl hydrazines [22,23]. These additions occur at the δ-meso position on the heme, while reactions of alkylhydrazines with myoglobin produce γ-meso alkylated hemes [24]. In each of these cases, the isoporphyrin is produced as a result of a free radical attack at a meso carbon on the porphyrin. A similar mechanism can easily be envisaged in the inactivation of $P450_{BM3}$-F87G by

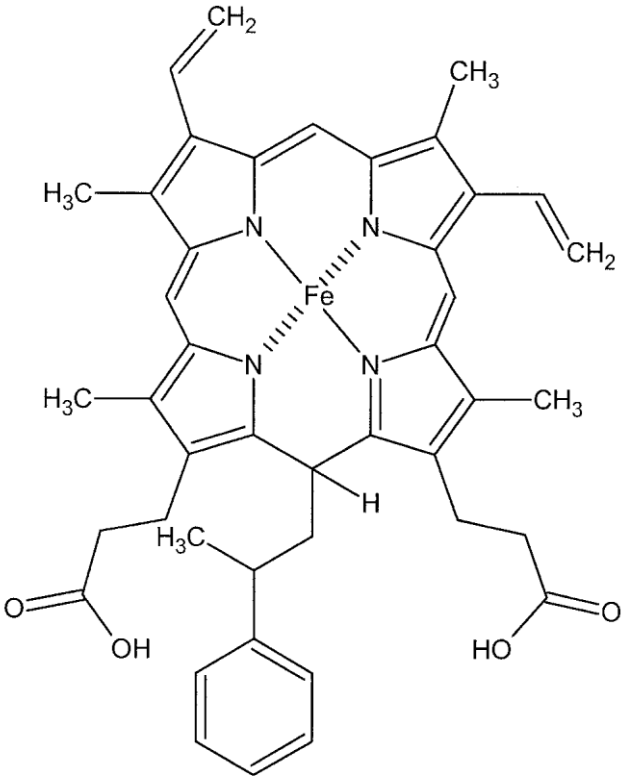

Fig. 8. Proposed isoporphyrin intermediate in the reaction of 3-PB and H_2O_2 with $P450_{BM3}$-F87G.

aldehydes, as the peroxo-pathway results in alkyl radical formation. Using 3PP, a phenylethyl radical is predicted, giving rise to a meso-phenylethyl-isoporphyrin species much like the one generated in studies by Ator et al. [21] using phenylethyl hydrazine and HRP.

Kinetic analysis of intermediate formation and decay using both 3PP and 3PB allowed us to assess the relative stability of the corresponding isoporphyrin intermediates. The rate of formation in each case was linearly dependent on the hydrogen peroxide concentration. The second order rate constants were $1.4X\ 10^{-2}$ and $1.02X\ 10^{-2}$ min^{-1} μM^{-1} for 3PB and 3PP, respectively. The data suggest that structural differences in the two aldehydes have little effect on the rate of activation, that is, deformylation with radical formation. The two substrates differ significantly, however, in the apparent deprotonation rate of their respective isoporphyrin intermediates. Here, the deprotonation refers to the loss of a proton from the γ-meso-carbon of the isoporphyrin. As H_2O_2 concentration increases, the k_2 values for each of the two aldehydes approaches a maximum value, indicative of a first order process, dependent only on the steady-state level of isoporphyrin present. Double reciprocal analysis of the data give the theoretical maximum values for k_2 of 1.07 and 6.0 min^{-1} for 3PB and 3PP, respectively. The sixfold lower k_2 for the 3PBdependent reaction, relative to that of the 3PP, is intriguing since the aldehydes differ by a single methyl group on C-2 of the propionyl chain, and k_2 presumably represents acid dissociation of the isoporphyrin. In an attempt to understand this difference in deprotonation rate, we examined the analogous heme modification in $P450_{2B4}$ with the intent of determining a value for k_2. For this isoform, heme adduct formation was observed, as described previously [5]; however, the reaction appeared to be monophasic, with no evidence for the formation of an isoporphyrin intermediate. Two factors may contribute to this observation; phase I of this reaction was slightly slower than phase I for the BM3 isoform. Secondly, phase II, which is suggested to be deprotonation of the isoporphyrin, may be substantially faster in 2B4. The combined effect of these would be masking of the isoporphyrin intermediate.

The difference in k_2 between $P450_{2B4}$ and $P450_{BM3}$- F87G is presumably the result of differences in their active site geometries, and the corresponding differences in the interactions between the isoporphyrin intermediate and the active site of the enzyme. For example, in BM3-F87G, the enhanced stability of the isoporphyrin may result

from strong binding interactions between the aldehyde phenyl group and the vacant Phe-87 site within the enzyme. This rationalization is illustrated in Scheme II. The phenylethyl radical produced in the deformylation of 3PP is ideally positioned for attack on the γ-meso carbon from above the plane of the porphyrin (Fig. 8), with the resulting formation of a putative isoporphyrin intermediate (step 1). According to the X-ray crystal structure, the formation of this intermediate would not require significant movement of the bound phenyl ring. However, for deprotonation to occur, the phenyl ring must move down toward the plane of the porphyrin in order to achieve the resulting aromatic heme structure (step 2). This may involve the extraction of the phenyl ring from its binding site, posing a kinetic barrier to deprotonation. If movement of the alkyl group toward the plane of the porphyrin influences intermediate stability, then it is a logical conclusion that as the steric bulk of the side chain increases, as is the case in going

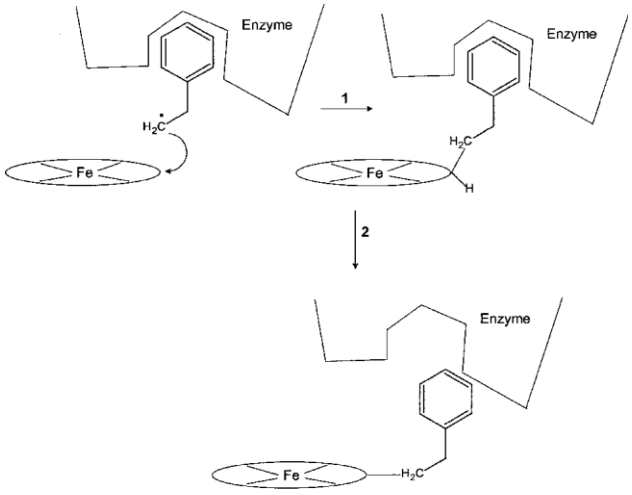

Scheme II.

from 3PP to 3PB, the rate of deprotonation should also decrease. Since the γ-meso carbon is flanked by propionate groups, the potential for steric interactions at this position is considerable. This model provides a qualitative explanation for the observed kinetics.

In conclusion, we report here the first direct evidence for an isoporphyrin intermediate in the inactivation of a cytochrome P450 enzyme. This proposed intermediate is mechanistically consistent with the observed alkylated heme product, and the intermediate spectra are very similar to those reported by Ator et al. [23] for isoporphyrin intermediates in the modification of horseradish peroxidase.

5. ABBREVIATIONS

2B4	cytochrome $P450_{2B4}$
BM3-F87G	cytochrome $P450_{BM3}$ with Phe-87 mutated to Gly
PA	phenylacetaldehyde
3PB	3-phenylbutyraldehyde
4PB	4-phenylbutyraldehyde
3PP	3-phenylpropionaldehyde
TFA	trifluoroacetic acid

ACKNOWLEDGEMENTS

This work was supported by Research Corporation Grant CC4924 to G.M.R. and National Institutes of Health Grant DK10339 to M.J.C.

REFERENCES

[1] C.A. Tyson, J.D. Lipscomb, I.C. Gunsalus, J. Biol. Chem. 247 (1972) 5777–5784.
[2] J.T. Groves, G.A. McClusky, R.E. White, M.J. Coon, Biochem. Biophys. Res. Commun. 81 (1978) 154–160.
[3] J.T. Groves, D.V. Subramanian, J. Am. Chem. Soc. 106 (1984) 2177–2181.
[4] A.D.N. Vaz, M.J. Coon, Biochemistry 33 (1994) 6442–6449.
[5] G.M. Raner, E.W. Chiang, A.D.N. Vaz, M.J. Coon, Biochemistry 36 (1997) 4895–4902.
[6] F.P. Guengerich, A.D.N. Vaz, G.M. Raner, S.J. Pernecky, M.J. Coon, Mol. Pharmacol. 51 (1997) 147–151.
[7] H.B. Dunford, in: J. Everse, K.E. Everse, M.B. Grisham (Eds.), Peroxidases in Chemistry and Biology, Vol. II, CRC Press, Boca Raton, FL, 1991, pp. 1–24.
[8] T. Egawa, H. Shimada, Y. Ishimura, Biochem. Biophys. Res. Commun. 201 (1994) 1464–1469.
[9] I. Schlichting, J. Berendzen, K. Chu, A.M. Stock, R.M. Sweet, D. Ringe, G.A. Petsko, M. Davies, E.J. Mueller, D. Benson, S. Sligar, FASEB J. 11 (1997) A769, Abstract.
[10] M. Akhtar, M.R. Calder, D.L. Corina, J.N. Wright, Biochem. J. 201 (1982) 569–580.
[11] E. S. Roberts, A.D.N. Vaz, M.J. Coon, Proc. Natl. Acad. Sci. USA 88 (1991) 8963–8966.
[12] A.D.N. Vaz, K.J. Kessell, M.J. Coon, Biochemistry 33 (1994) 13651–13661.
[13] A.D.N. Vaz, S.J. Pernecky, G.M. Raner, M.J. Coon, Biochemistry 93 (1996) 4644–4648.
[14] C.-L. Kuo, G.M. Raner, A.D.N. Vaz, M.J. Coon, Biochemistry 38 (1999) 10511–10518.
[15] H. Li, T.L. Poulos, Acta Crystallogr. Sect. D 51 (1995) 21.
[16] S. Graham-Lorence, G. Truan, J.A. Peterson, J.R. Falck, S. Wei, C. Gelvig, J.H. Capdevila, J. Biol. Chem. 272 (1997) 1127–1135.
[17] U. Schwaneberg, C. Schmidt-Dannert, J. Schmitt, R.D. Schmid, Anal. Biochem. 269 (1999) 359–366.
[18] S.C. Davis, Z. Sui, J.A. Peterson, P.R. Ortiz de Montellano, Arch. Biochem. Biophys. 328 (1996) 35–42.
[19] S.S. Boddupalli, R.W. Estabrook, J.A. Peterson, J. Biol. Chem. 265 (1990) 4233–4239.
[20] T. Omura, R. Sato, J. Biol. Chem. 239 (1964) 2379–2385.
[21] M.A. Ator, S.K. David, P.R. Ortiz de Montellano, J. Biol. Chem. 262 (1987) 14954–14960.
[22] J.S. Wiseman, J.S. Nichols, M.X. Kolpak, J. Biol. Chem. 257 (1982) 6328–6332.
[23] M.A. Ator, S.K. David, P.R. Ortiz de Montellano, J. Biol. Chem. 264 (1989) 9250–9257.
[24] Y.S. Choe, P.R. Ortiz de Montellano, J. Biol. Chem. 266 (1991) 8523–8530.